

Thus, the Bni1p FH2 domain is an actin nucleator with unique properties for polarizing growing filaments. In vitro, Bni1pFH1FH2 stimulates assembly of unbranched filaments and associates with their barbed ends, yet still permits barbed-end growth. In vivo, yeast formins direct assembly of actin cables (7, 8) that radiate from discrete regions of the growing cell cortex (28) where the formins are localized (2, 29–31). Unidirectional movements of a cable-dependent myosin-V indicate that cable filaments are oriented with their barbed ends directed toward the growing cortex (32), and in vivo actin cable dynamics have shown that cables assemble at these sites (33). Our observations suggest that Bni1p directly nucleates cable filaments and tethers them by their growing barbed ends, establishing their polarity. Conservation of this mechanism may explain the roles of formins in the assembly of unbranched filamentous actin arrays in other eukaryotes.

References and Notes

1. H. Kohno et al., *EMBO J.* **15**, 6060 (1996).
2. M. Evangelista et al., *Science* **276**, 118 (1997).
3. H. Imamura et al., *EMBO J.* **16**, 2745 (1997).
4. A. J. Ridley, *Nature Cell Biol.* **1**, E64 (1999).
5. S. Wasserman, *Trends Cell Biol.* **8**, 111 (1998).
6. R. Zeller et al., *Cell Tissue Res.* **296**, 85 (1999).
7. M. Evangelista, D. Pruyne, D. C. Amberg, C. Boone, A. Bretscher, *Nature Cell Biol.* **4**, 32 (2002).
8. I. Sagot, S. K. Klee, D. Pellman, *Nature Cell Biol.* **4**, 42 (2002).
9. D. W. Pruyne, D. H. Schott, A. Bretscher, *J. Cell Biol.* **143**, 1931 (1998).
10. K. L. Hill, N. L. Catlett, L. S. Weisman, *J. Cell Biol.* **135**, 1535 (1996).
11. C. L. Theesfeld, J. E. Irazoqui, K. Bloom, D. J. Lew, *J. Cell Biol.* **146**, 1019 (1999).
12. O. W. Rossanese et al., *J. Cell Biol.* **153**, 47 (2001).
13. D. Hoepfner, M. van den Berg, P. Philippsen, H. F. Tabak, E. H. Hetterma, *J. Cell Biol.* **155**, 979 (2001).
14. D. C. Winter, E. Y. Choe, R. Li, *Proc. Natl. Acad. Sci. U.S.A.* **96**, 7288 (1999).
15. The following supplementary materials are available on Science Online: a description of materials and methods and a note providing further discussion of the defects of CB on nucleation by GST-Bni1pFH1FH2, and fig. S1.
16. D. Pruyne et al., data not shown.
17. L. M. Machesky et al., *Proc. Natl. Acad. Sci. U.S.A.* **96**, 3739 (1999).
18. D. H. Castrillon, S. A. Wasserman, *Development* **120**, 3367 (1994).
19. S. Emmons et al., *Genes Dev.* **9**, 2482 (1995).
20. The domain organization of Bni1p was based on the analysis of 75 formin orthologs accessed through the Pfam database of protein domains (<http://pfam.wustl.edu/index.html>).
21. S. MacLean-Fletcher, T. D. Pollard, *Cell* **20**, 329 (1980).
22. D. C. Lin, S. Lin, *Anal. Biochem.* **103**, 316 (1980).
23. J. A. Cooper et al., *J. Cell Biol.* **104**, 491 (1987).
24. R. Tellam, C. Frieden, *Biochemistry* **21**, 3207 (1982).
25. T. D. Pollard, L. Blanchoin, R. D. Mullins, *Annu. Rev. Biophys. Biomol. Struct.* **29**, 545 (2000).
26. J. R. Glenney Jr., P. Kaulfus, K. Weber, *Cell* **24**, 471 (1981).
27. J. E. Caldwell, S. G. Heiss, V. Mermall, J. A. Cooper, *Biochemistry* **28**, 8506 (1989).
28. A. E. Adams, J. R. Pringle, *J. Cell Biol.* **98**, 934 (1984).
29. R. P. Jansen, C. Dowzer, C. Michaelis, M. Galova, K. Nasmyth, *Cell* **84**, 687 (1996).
30. T. Kamei et al., *J. Biol. Chem.* **273**, 28341 (1998).
31. K. Ozaki-Kuroda et al., *Mol. Cell Biol.* **21**, 827 (2001).
32. D. H. Schott, R. N. Collins, A. Bretscher, *J. Cell Biol.* **156**, 35 (2002).

33. H. C. Yang, L. A. Pon, *Proc. Natl. Acad. Sci. U.S.A.* **99**, 751 (2002).
34. We thank M. Johnson and M. Strang for assistance with the electron microscopy; C. Koth, R. Adorn-Broza, B. Kus, and A. Edwards for advice on protein purification of GST-Bni1 fragments; A. Davidson for valuable time on his spectrofluorometer; H. Zhu and M. Joyce for technical assistance; and S. Kim, D. Schott, and M. Tyers for critical reading and assistance with the manuscript. Supported by NIH grants AI19883 (S.Z.), GH39066 (D.P. and A.B.), and GM59216 (E.B.); a National Cancer Institute of Can-

ada (NCIC) grant (C.B.); and an NCIC graduate student fellowship (M.E.).

**Supporting Online Material**  
[www.sciencemag.org/cgi/content/full/1072309/DC1](http://www.sciencemag.org/cgi/content/full/1072309/DC1)  
 Materials and Methods  
 Fig. S1  
 References S1 to S5

28 March 2002; accepted 27 May 2002  
 Published online 6 June 2002;  
 10.1126/science.1072309  
 Include this information when citing this paper.

## Modulation of Postendocytic Sorting of G Protein–Coupled Receptors

Jennifer L. Whistler,<sup>1\*</sup> Johan Enquist,<sup>2</sup> Aaron Marley,<sup>3</sup> Jamie Fong,<sup>1</sup> Fredrik Gladher,<sup>2</sup> Pamela Tsuruda,<sup>3</sup> Stephen R. Murray,<sup>3</sup> Mark von Zastrow<sup>3\*</sup>

Recycling of the mu opioid receptor to the plasma membrane after endocytosis promotes rapid resensitization of signal transduction, whereas targeting of the delta opioid receptor (DOR) to lysosomes causes proteolytic down-regulation. We identified a protein that binds preferentially to the cytoplasmic tail of the DOR as a candidate heterotrimeric GTP-binding protein (G protein)–coupled receptor-associated sorting protein (GASP). Disruption of the DOR-GASP interaction through receptor mutation or overexpression of a dominant negative fragment of GASP inhibited receptor trafficking to lysosomes and promoted recycling. The GASP family of proteins may modulate lysosomal sorting and functional down-regulation of a variety of G protein–coupled receptors.

Ligand-induced endocytosis contributes to the physiological regulation of a wide variety of signaling receptors. Many G protein–coupled receptors (GPCRs) are endocytosed by a mechanism involving receptor phosphorylation, interaction with nonvisual (beta-) arrestins, and concentration in clathrin-coated pits [reviewed in (1, 2)]. However, the functional consequences of GPCR endocytosis through this conserved cellular mechanism are diverse. Trafficking of internalized GPCRs by a rapid recycling pathway restores the complement of functional receptors in the plasma membrane and promotes resensitization of receptor-mediated signal transduction (1, 3, 4). In contrast, the sorting of internalized GPCRs to lysosomes promotes proteolytic down-regulation of receptors, leading to a prolonged attenuation of cellular signal transduction (3, 5, 6). Furthermore, the post-endocytic sorting of certain GPCRs can itself be regulated under physiological conditions (7).

Mu opioid receptors (MORs) and DORs

are structurally homologous GPCRs that mediate the actions of endogenously produced opioid neuropeptides and exogenously administered opiate drugs. Both receptors are endocytosed via clathrin-coated pits after agonist-induced activation, phosphorylation, and association with cytoplasmic beta-arrestins (8, 9). However, previous studies suggest that endocytosis causes different effects on MOR as compared to DOR (6, 10–12). A FLAG epitope–tagged DOR [DOR-1 (13)] expressed in stably transfected human embryonic kidney (HEK) 293 cells (14) exhibited pronounced down-regulation within 3 hours of exposure to opioid peptide agonist, whereas FLAG-tagged MOR [MOR-1 (15)] expressed at similar levels did not down-regulate (Fig. 1A) (16). A biochemical assay that specifically measures the fate of surface-biotinylated receptors (12, 17, 18) indicated that DOR but not MOR was rapidly proteolyzed after agonist-induced endocytosis (Fig. 1B). Fluorescence microscopy indicated that exposure of cells to agonist for 90 min caused DORs to concentrate in membranes located in the perinuclear region of the cells, many of which colocalized with the late endosome and lysosome markers LAMP1 and LAMP2 (Fig. 1C) (19). In contrast, MOR was localized under these conditions in vesicles distributed throughout the cytoplasm that failed to colocalize substantially with LAMP1 and

<sup>1</sup>Department of Neurology, Ernest Gallo Clinic and Research Center, University of California, San Francisco, Emeryville, CA 94608, USA. <sup>2</sup>Program in Molecular Medicine, University of Lund, Sweden. <sup>3</sup>Program in Cell Biology, Department of Psychiatry and Department of Cellular and Molecular Pharmacology, University of California, San Francisco, CA 94143, USA.

\*To whom correspondence should be addressed. E-mail: shooz2@itsa.ucsf.edu (J.L.W.); zastrow@itsa.ucsf.edu (M.v.Z.)

LAMP2 (Fig. 1C). Replacing the cytoplasmic tail of MOR with the corresponding sequence from the cytoplasmic tail of DOR enhanced down-regulation of ligand-binding sites and postendocytic proteolysis of a chimeric mutant MOR [degrading MOR (D MOR)] after endocytosis induced by opioid peptide or the highly potent alkaloid agonist etorphine (Fig. 1, A and B), as shown previously for this mutant receptor after morphine-induced endocytosis (12). Conversely, replacing a por-

tion of the DOR tail with the corresponding sequence derived from MOR inhibited post-endocytic proteolysis of a chimeric mutant DOR [recycling DOR (R DOR)] (Fig. 1B) (20). Furthermore, differences in postendocytic trafficking conferred by exchanging the DOR tail were associated with significant effects on the ability of receptors to be functionally resensitized after prolonged agonist stimulation of cells (Fig. 1D) (9, 21). Thus, the DOR tail could contain a signal that is not

conserved in MOR and controls a functionally important sorting decision that leads to receptor trafficking to lysosomes.

We next sought to identify tail-interacting proteins that could modulate sorting of DOR. A yeast two-hybrid screen of an HEK293 cell-derived cDNA library using the DOR tail domain as the bait (22) yielded multiple clones corresponding to various COOH-terminal portions of a large predicted protein, whose mRNA is expressed in many tissues and is enriched in the brain (23). A full-length cDNA (KIAA0443) encoding a 1395-residue predicted protein was obtained from the Kazusa DNA Research Institute (23). Affinity chromatography using glutathione *S*-transferase (GST) fusion proteins confirmed that the cloned interacting protein bound specifically to the DOR tail and not to the GST that lacked the tail sequence (Fig. 2A) (24). This protein bound much more weakly to the cytoplasmic tail of MOR (Fig. 2A) and R DOR (25), consistent with a potential function in modulating DOR trafficking. We named this protein GASP for candidate G protein-coupled receptor-associated sorting protein. Psi-BLAST searches conducted with the GenBank database indicated that GASP is a previously unknown protein with human, rat, and murine homologs (26).

An antibody to the COOH-terminal 15 residues of GASP (27) recognized a major immunoreactive protein in immunoblots of (untransfected) HEK293 cell lysates, which had similar electrophoretic mobility to recombinant hemagglutinin (HA)-tagged GASP expressed in HEK293 cells (Fig. 2B) or produced by *in vitro* translation (Fig. 2A) (28, 29). We used this antibody to assess whether endogenous GASP and DOR interact *in vivo*. Although antibody staining of endogenous GASP in fixed cells was not detected using fluorescence microscopy, recombinant GASP [tagged with HA or green fluorescent protein (GFP)] localized throughout the cytoplasm in transfected cells. A fraction of the endogenous GASP present in HEK293 cell lysates coimmunoprecipitated specifically with full-length DOR but not with MOR expressed at similar levels (Fig. 2C) (30). Conversely, DOR coimmunoprecipitated with endogenously expressed GASP, confirming the occurrence and specificity of the receptor-GASP interaction in intact cells (Fig. 2D).

GST affinity chromatography was used to identify a COOH-terminal fragment of GASP (cGASP, corresponding to the COOH-terminal 497 residues of GASP) that bound specifically to the DOR tail, consistent with the finding that several two-hybrid hits contained this portion of GASP (Fig. 3A). cGASP bound to the DOR tail with an apparent affinity comparable to that of full-length GASP (Fig. 3B) (24), as indicated by the similar

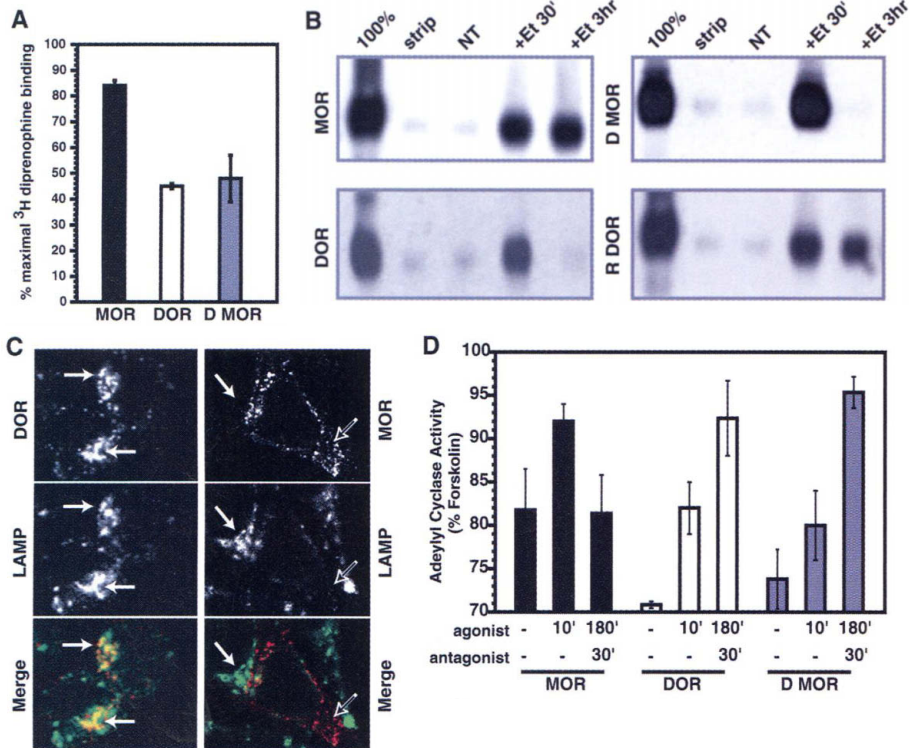


**Fig. 1.** Postendocytic trafficking of opioid receptors. (A) Agonist-induced down-regulation of opioid receptors. Cells stably expressing MOR, DOR, or D MOR (~1 to 2 pmol/mg) were either incubated in the presence of the opioid peptide agonist for 3 hours or left untreated. Cells were then chilled on ice and washed extensively, and total opioid radioligand binding sites were determined for each cell line (16). Both DOR and D MOR showed significant down-regulation, whereas MOR was not substantially down-regulated under the same conditions ( $P < 0.001$ ). Error bars represent SD from a representative experiment ( $n = 3$  experiments), with each data point derived from triplicate determinations. (B) Postendocytic sorting of MOR, DOR, D MOR, and R DOR was analyzed by biotin protection-degradation, which selectively follows the stability of endocytosed receptor protein (12, 17, 18). Endocytosed DOR and D MOR were extensively proteolyzed after 3 hours of agonist treatment, whereas endocytosed MOR and R DOR were stable. + ET 3 hour, exposure to the agonist etorphine for 3 hours; + ET 30', exposure to the agonist etorphine for 30 min; NT, nontreated. Blots are representative of at least two independent experiments. (C) Internalized DOR was colocalized with the late endosome and lysosomal markers LAMP1 and LAMP2 after 90 min of agonist [5  $\mu$ M [D-Ala<sup>2</sup>, D-Leu<sup>5</sup>] enkephalin (DADLE)] incubation (19), whereas MOR was not colocalized with LAMPs after 90 min of agonist [5  $\mu$ M [D-Ala<sup>2</sup>, N-Me Phe<sup>4</sup>, Gly-ol<sup>5</sup>] -enkephalin (DAMGO)]. Solid arrows, areas of the cells concentrated in LAMP. Open arrows, areas where MOR is distributed in areas without LAMP. (D) Functional effects of opioid receptor membrane trafficking on signal transduction were assessed by a membrane adenylyl cyclase assay (21) from stably transfected cells expressing MOR, DOR, or D MOR. Rapid desensitization of all three receptors was observed after a brief (10 min) exposure of cells to agonist (5  $\mu$ M DAMGO for MOR and D MOR, 5  $\mu$ M DADLE for DOR). Significant differences were observed between cell lines after pretreatment with agonist for 3 hours and then agonist washout and subsequent incubation with opiate antagonist (10  $\mu$ M naloxone) for 30 min. MOR-expressing cells recovered their ability to mediate agonist-dependent inhibition of adenylyl cyclase, consistent with resensitization of receptors mediated by recycling (17). In contrast, neither DOR nor D MOR resensitized significantly under similar conditions, consistent with the postendocytic sorting to lysosomes and the subsequent down-regulation of these receptors (6, 12). Error bars represent SD from a representative experiment ( $n = 2$  experiments), with each data point derived from triplicate determinations.

fraction of GASP and cGASP recovered on beads when applied at similar concentrations and assayed by parallel GST binding (Figs. 2A and 3B). A GFP-tagged version of cGASP stably overexpressed in HEK293 cells coimmunoprecipitated with wild-type DOR but not MOR (Fig. 3C) (30), demonstrating that the specificity of the cGASP-DOR interaction observed in intact cells parallels that of the DOR-GASP interaction observed *in vitro*. cGASP was able to compete for binding of full-length GASP to the DOR tail *in vitro* (Fig. 3D) (31). Furthermore, GFP-cGASP, when highly overexpressed (Fig. 3E), markedly reduced the amount of endogenous GASP recovered in DOR immunoprecipitates (Fig. 3E), suggesting that cGASP can function in intact cells as a dominant inhibitor of the interaction between endogenous GASP and DOR.

To begin to examine the role of GASP in mediating sorting of DOR in intact cells, an HA-tagged cGASP construct was expressed by transient transfection in cells stably expressing FLAG-tagged DOR. Trafficking of antibody-labeled receptors was examined by fluorescence microscopy, and dual-color labeling was used to identify cGASP-transfected cells in the cell population (19). Cells overexpressing cGASP showed robust internalization of DOR in response to the agonist, which was similar to that observed in adjacent cells in the specimen not expressing cGASP (Fig. 4A). However, after agonist washout, an increased amount of DOR immunoreactivity was seen in the plasma membrane of cells expressing HA-cGASP as compared to those that did not (Fig. 4A). Thus, cGASP could function as a dominant inhibitor of postendocytic sorting of DOR, consistent with the ability of cGASP to compete with full-length or endogenous GASP for binding to DOR both *in vitro* (Fig. 3D) and *in vivo* (Fig. 3E).

A dominant negative effect of cGASP on lysosomal sorting of DOR was also suggested by studies examining the localization of internalized DOR relative to the late endosome and lysosome markers LAMP1 and LAMP2. In cGASP-overexpressing cells, internalized DOR exhibited reduced colocalization with LAMP after 90-min exposure to the agonist (Fig. 4B) as compared to the DOR in cells expressing only endogenous GASP (Fig. 1C) (19). The effects of cGASP were further examined using the biotin protection-degradation assay (12, 17, 18). In cells overexpressing cGASP, we observed a detectable fraction of internalized DOR that was not proteolyzed even after continuous incubation of cells in the presence of agonist for 3 hours (Fig. 4C). Agonist-induced down-regulation of DOR (measured by radioligand binding assay) was also inhibited in cells overexpressing cGASP (Fig. 4E), and the extent of

**Fig. 2.** GASP binding to opioid receptors. (A) Recombinant GASP produced by *in vitro*-translation bound selectively to a GST fusion protein containing the cytoplasmic tail of DOR and to MOR with much reduced affinity (24). (B) An antibody to a GASP peptide (27) recognized an endogenous protein in HEK293 cells that coelectrophoresed with recombinantly expressed HA-tagged GASP. IB, immunoblot. Lysates were separated by SDS-PAGE and transferred to nitrocellulose, and the blot was cut in half before immunoblotting with antibodies to HA and GASP.

(C) GASP selectively bound to DOR but not MOR *in vivo* (30). Cells stably expressing MOR, DOR (~1 to 2 pmol/mg), or no receptor were lysed, and receptors were immunoprecipitated. Precipitates were immunoblotted for GASP (upper blot) and receptor (middle blot). Lower blot shows lysate samples immunoblotted for GASP. Less than 1% of endogenous GASP was immunoprecipitated with DOR. IP, immunoprecipitate. (D) DOR bound GASP *in vivo*. HEK293 cells or HEK293 cells stably expressing DOR were lysed and GASP was immunoprecipitated. Precipitates were immunoblotted for receptor. Less than 1% of the total DOR was recovered in the GASP immunoprecipitate; nevertheless, coimmunoprecipitations conducted in both directions were highly specific.

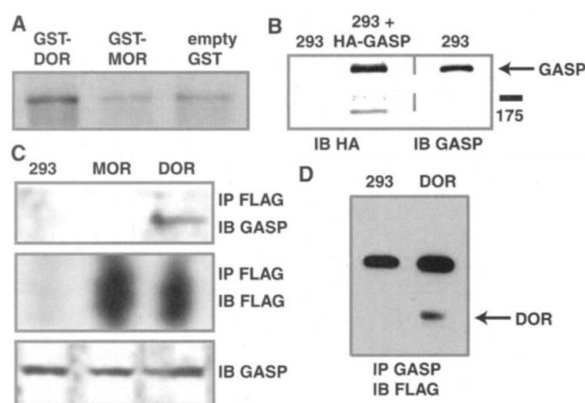
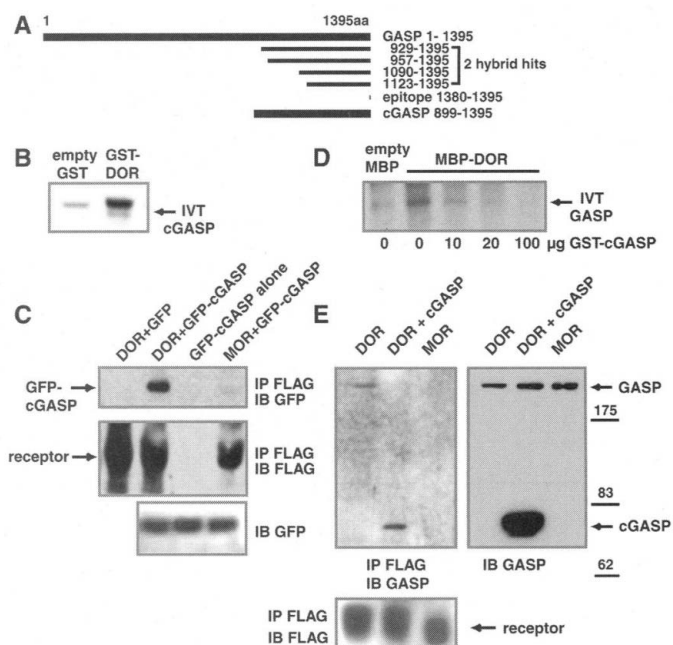


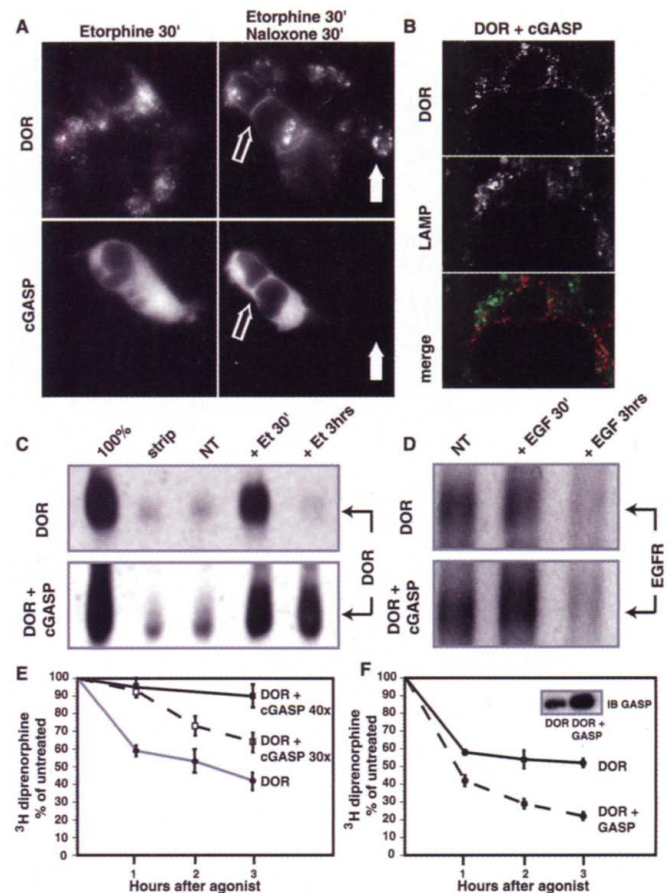
**Fig. 3.** cGASP binding to opioid receptors.

(A) Diagram showing the GASP hits from the two-hybrid screen, the extent of cGASP, and the epitope used to prepare an antibody to GASP. aa, amino acid. (B) DOR bound to cGASP *in vitro* (IVT) (24). Approximately 3 to 5% of the input cGASP was recovered on washed GST-DOR. (C) GFP-cGASP bound to DOR but not MOR *in vivo* (30). Cells stably expressing GFP-cGASP alone, GFP-cGASP and FLAG-tagged DOR, or MOR were lysed, and receptors were immunoprecipitated with antibody to FLAG. Precipitates were immunoblotted specifically



for cGASP using antibodies to GFP (upper blot) or opioid receptor using antibody to FLAG (middle blot). Lower blot shows samples of cell lysate immunoblotted for GFP-cGASP. Cells stably expressing both DOR and (wild-type) GFPs were analyzed in parallel to ensure DOR was not coimmunoprecipitating with GFP. (D) cGASP competed for binding of full-length GASP to the DOR tail *in vitro*. Bacterially expressed MBP-DOR or MBP-lacZ ("empty MBP") was immobilized to amylose resin. *In vitro*-translated full-length GASP bound specifically to the MBP-DOR tail. Additions of bacterially expressed and purified GST-cGASP competed for binding of full-length GASP to MBP-DOR in a concentration-dependent manner (31). (E) GFP-cGASP competed with endogenous GASP for binding to DOR *in vivo* (30). Opioid receptors were immunoprecipitated from cells stably expressing FLAG-DOR alone, FLAG-DOR and GFP-cGASP, or FLAG-MOR. Precipitates were blotted for GASP using the anti-GASP peptide antibody to detect endogenous GASP and expressed cGASP (left blot), or for opioid receptor using anti-FLAG antibody (lower blot). Lysate samples were immunoblotted for GASP (right blot), demonstrating that cGASP was overexpressed approximately 40-fold over endogenous GASP. Immunoprecipitates were normalized for receptor (to assess the amount of GASP binding per receptor), not total protein; hence slight differences in total GASP immunoreactivity were noted between lanes. A small percentage (<1%) of the total amount of endogenous GASP was coimmunoprecipitated with DOR in cells not overexpressing cGASP. In cells overexpressing cGASP, no detectable endogenous GASP was detected in receptor immunoprecipitates, but cGASP (also <1% of total present in the cell lysate) coimmunoprecipitated with DOR.

**Fig. 4.** cGASP was a dominant inhibitor of DOR sorting to lysosomes. **(A)** cGASP overexpression facilitated DOR recycling. Cells stably expressing FLAG-DOR were transiently transfected with HA-tagged-cGASP, and cells were treated either with agonist for 30 min (left panels) or agonist for 30 min followed by agonist washout and subsequent incubation with antagonist for 30 min (right panels). Endocytic trafficking of antibody-labeled DOR was examined by fluorescence microscopy (19). cGASP had no visible effect on agonist-induced endocytosis of receptors (left panels; numerous endocytic vesicles containing antibody-labeled DOR were observed in adjacent cells with and without overexpression of cGASP). However, cGASP did affect receptor trafficking after agonist washout. In cells not overexpressing cGASP (right panels, solid arrows), antibody-labeled DOR remained predominantly in endocytic vesicles after agonist washout, consistent with efficient sorting of this receptor out of a rapid recycling pathway (6). In contrast, in cells overexpressing cGASP (right panels, open arrows) an increased amount of DOR was observed in the plasma membrane after agonist washout, suggesting increased recycling of internalized DOR. **(B)** cGASP effect on localization of DOR in lysosomes. Stably transfected cells expressing both FLAG-DOR and HA-cGASP (all cells express both) were treated with opioid peptide agonist (5  $\mu$ M DADLE) for 90 min and stained for receptor and the late endosome and lysosomal markers LAMP1 and LAMP2. Little colocalization of internalized DOR and LAMPs was observed (19), in contrast to the substantial colocalization observed under similar conditions in cells not overexpressing cGASP (Fig. 1C). **(C)** cGASP inhibited postendocytic proteolysis of DOR. The postendocytic trafficking of DOR was assessed in cells stably expressing DOR alone or both DOR and GFP-cGASP using a biotin protection-degradation assay to selectively follow the stability of endocytosed receptors (12, 17, 18). Endocytosed DOR was completely degraded within 3 hours after agonist addition to cells not overexpressing cGASP, whereas biotinylated DOR was much more stable in cells overexpressing cGASP. **(D)** EGF receptor degradation was not inhibited by cGASP overexpression. Stably transfected cells expressing FLAG-DOR or FLAG-DOR together with GFP-cGASP were either left untreated or incubated with EGF (5  $\mu$ M) for 30 min or 3 hours. Endogenously expressed EGF receptor was immunoprecipitated and analyzed by SDS-PAGE and immunoblot (32). Overexpression of cGASP did not detectably inhibit proteolysis of the EGF receptor. **(E)** cGASP inhibited agonist-induced down-regulation of DOR as measured by radioligand binding. Cells stably expressing DOR alone or DOR and cGASP were either treated with agonist (5  $\mu$ M DADLE) for 1 to 3 hours or left untreated. Cells were then washed extensively to remove residual agonist, and total ligand-binding sites present in cell lysates were determined (16). Agonist-induced down-regulation of DOR was significantly inhibited in cells overexpressing cGASP 40 times more than endogenous GASP ( $P < .001$ ) and less significantly in cells that overexpressed cGASP only 30 times more than endogenous GASP ( $P < .05$ ). Error bars as in Fig. 1A ( $n = 3$  experiments). **(F)** Overexpression of full-length GASP enhanced DOR down-regulation. Cells stably expressing FLAG-DOR together with an NH<sub>2</sub>-terminal GFP-tagged full-length GASP or expressing DOR alone were either left untreated or treated with agonist (5



$\mu$ M DADLE) for 1, 2, or 3 hours. Cells were then washed extensively to remove residual agonist, and the total number of ligand-binding sites present in cell lysates was determined (16). Data points, mean number of opioid binding sites; error bars are as in (E). Agonist-induced down-regulation of DOR was significantly enhanced both in rate and in extent in cells overexpressing GASP. Inset shows an immunoblot of cell lysates using GASP antibodies demonstrating ~4-fold overexpression of GASP in these cells relative to endogenous levels. We were unable to obtain viable cell clones expressing higher levels of full-length GASP.

inhibition correlated with the overexpression of cGASP. However, ligand-induced proteolysis of epidermal growth factor (EGF) receptors, a distinct class of receptor tyrosine kinases that are expressed endogenously in these cells and traffic to lysosomes after agonist-induced endocytosis, was not inhibited in cells overexpressing cGASP (Fig. 4D) (32). Thus, overexpression of cGASP specifically inhibited the sorting of DOR to lysosomes without affecting the trafficking of a structurally distinct receptor that follows a similar endocytic pathway.

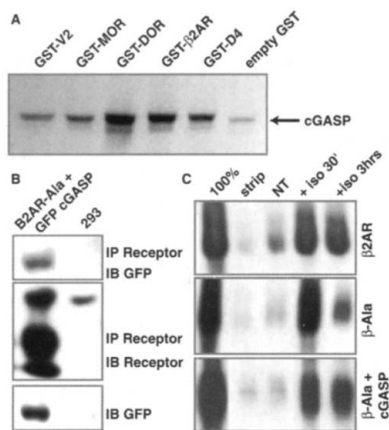
The most dramatic effects on DOR trafficking and down-regulation were observed in cell clones overexpressing cGASP at high levels (>30 times that of the endogenous GASP) (Fig. 4E), suggesting that the dominant negative cGASP function is antimorphic. However, cGASP might have exerted its dominant negative effect on DOR sorting not because it blocked DOR binding to en-

dogenous GASP, but because it blocked DOR binding to a different protein or had other cellular effects. In this case, we predicted that overexpression of full-length GASP, which also bound to DOR in vitro and in vivo, would inhibit DOR sorting to lysosomes. It was difficult to generate cell lines that stably overexpress full-length GASP at high levels. Several rounds of selection and subcloning produced a cell line that stably overexpressed a GFP-tagged version of full-length GASP about 4 times more than endogenous GASP levels (Fig. 4F). These cells had a doubling time about 3 times that of cell clones of DOR-HEK293 that express endogenous levels of GASP or overexpress cGASP, suggesting that overexpression of full-length GASP was not well tolerated. Nevertheless, in these cells down-regulation of DOR was not inhibited but was significantly enhanced (Fig. 4F). Although we cannot rule out additional effect(s) of full-length

GASP on cell growth or viability, these results suggest that cGASP affects DOR trafficking by specifically inhibiting the binding of DOR to endogenous GASP and support the hypothesis that GASP is indeed a sorting protein that modulates trafficking of internalized DOR to lysosomes.

We next examined whether GASP might modulate the endocytic sorting of other (non-opioid) GPCRs. A limited survey using GST affinity chromatography indicated that cGASP interacted with the cytoplasmic tails of catecholamine receptors such as the  $\beta$ -2 adrenergic receptor ( $\beta_2$ AR) and the D4 dopamine receptor (Fig. 5A). We also observed high levels of binding to the cytoplasmic tail of the  $\alpha$ -2B adrenergic receptor, which has been shown previously to undergo agonist-induced proteolysis (33). In contrast, cGASP (and GASP) bound only weakly to the MOR tail and did not bind at all (over nonspecific background levels) to the cytoplasmic tail of

**Fig. 5.** Interaction of GASP with other GPCRs. **(A)** Affinity chromatography was used to estimate binding of in vitro–translated cGASP to GST fusion proteins corresponding to the cytoplasmic tails of several GPCRs (24). cGASP (like full-length GASP) bound strongly to the DOR tail and weakly to the MOR tail. cGASP bound to the cytoplasmic tail of the  $\beta_2$ AR nearly as strongly as to DOR. A high amount of binding over background (“empty GST”) and GST-MOR levels was also observed to the human D4 dopamine receptor tail but not to the V2 vasopressin receptor tail. **(B)** GFP-cGASP bound in vivo to a mutant form of the  $\beta_2$ AR,  $\beta_2$ AR-Ala, that is sorted to lysosomes after endocytosis (7). HA- $\beta_2$ AR-Ala and GFP-cGASP were coexpressed in stably transfected cells, and receptors were immunoprecipitated using antibodies to HA. Precipitates were blotted using antibodies to GFP to detect the cGASP construct (upper blot) or antibodies to FLAG to detect receptor (middle blot). Lower blot shows lysate samples immunoblotted for GFP-cGASP (30). **(C)** cGASP inhibited postendocytic proteolysis of  $\beta_2$ AR-Ala. The postendocytic trafficking of  $\beta_2$ AR was assessed in cells stably expressing  $\beta_2$ AR alone,  $\beta_2$ AR-Ala alone, or  $\beta_2$ AR-Ala and c-GASP by using the biotin protection-degradation assay to selectively follow the stability of endocytosed receptors (12, 17, 18). cGASP overexpression increased the recovery of intact, biotinylated receptors from cells after exposure to the adrenergic agonist isoproterenol (iso, 10  $\mu$ M) for 3 hours.



the V2 vasopressin receptor (Fig. 5A). The lack of GASP interaction with the V2 receptor tail is consistent with the remarkable ability of these receptors to remain in endocytic vesicles for a prolonged period of time after endocytosis without undergoing any detectable down-regulation (34). The ability of GASP to bind to the  $\beta_2$ AR tail in vitro was initially surprising because  $\beta_2$ AR recycles efficiently after agonist-induced endocytosis and is relatively resistant to proteolysis in HEK293 cells (35). However, efficient recycling of the  $\beta_2$ AR in these cells requires a distinct set of protein interactions with the distal tip of the cytoplasmic tail (7, 36, 37), which is thought to be a point of physiological regulation and is disrupted in a mutant  $\beta_2$ AR ( $\beta_2$ AR-Ala) that trafficks rapidly to lysosomes after agonist-induced endocytosis (7). Hence we considered that cGASP might also interact in vivo with the  $\beta_2$ AR-Ala mutant receptor and modulate its sorting to lysosomes. Consistent with this, GFP-cGASP coimmunoprecipitated with  $\beta_2$ AR-Ala (Fig. 5B) (30). Furthermore, overexpression of GFP-cGASP inhibited degradation of internalized  $\beta_2$ AR-Ala (Fig. 5C).

Thus, GASP is a cytoplasmic protein that interacts selectively with a subset of GPCRs and modulates their endocytic sorting to lysosomes. Certain GPCRs are targeted to lysosomes by a conserved mechanism involving covalent modification of the cytoplasmic tail by ubiquitin (38–40). Previous studies have implicated ubiquitinylation of DOR specifically in targeting receptors to proteasomes (41) but not in receptor trafficking to lysosomes (42), and our in vitro data suggest that GASP binds to the nonubiquitinylated DOR tail. Despite the ability of GASP to bind to the nonubiquitinylated  $\beta_2$ AR tail in vitro and

modulate the trafficking of a mutant  $\beta_2$ AR to lysosomes in vivo, it is interesting that down-regulation of the  $\beta_2$ AR in mammalian cells has been shown recently to be modulated by ubiquitinylation (40). Therefore, it is possible that multiple mechanisms, involving both covalent modification of the receptor itself and noncovalent interactions with proteins such as GASP, control the sorting of endocytosed GPCRs in mammalian cells. Such complexity in the postendocytic sorting machinery might be critical for generating the remarkable diversity and specificity with which signaling receptors are regulated in multicellular organisms.

**References and Notes**

1. A. Claing, S. A. Laporte, M. G. Caron, R. J. Lefkowitz, *Prog. Neurobiol.* **66**, 61 (2002).
2. O. B. Goodman Jr. et al., *Adv. Pharmacol.* **42**, 429 (1998).
3. J. Trejo, S. R. Coughlin, *J. Biol. Chem.* **274**, 2216 (1999).
4. R. J. Lefkowitz, J. Pitcher, K. Krueger, Y. Daaka, *Adv. Pharmacol.* **42**, 416 (1998).
5. A. W. Gagnon, L. Kallal, J. L. Benovic, *J. Biol. Chem.* **273**, 6976 (1998).
6. P. I. Tsao, M. von Zastrow, *J. Biol. Chem.* **275**, 11130 (2000).
7. T. T. Cao, H. W. Deacon, D. Reczek, A. Bretscher, M. von Zastrow, *Nature* **401**, 286 (1999).
8. J. Zhang et al., *Proc. Natl. Acad. Sci. U.S.A.* **95**, 7157 (1998).
9. J. Zhang et al., *J. Rec. Sig. Trans. Res.* **19**, 1 (1999).
10. P. Y. Law, H. H. Loh, *J. Pharmacol. Exp. Ther.* **289**, 607 (1999).
11. T. Koch et al., *J. Biol. Chem.* **273**, 13652 (1998).
12. A. K. Finn, J. L. Whistler, *Neuron* **32**, 829 (2001).
13. C. J. Evans, D. E. Keith Jr., H. Morrison, K. Magendzo, R. H. Edwards, *Science* **258**, 1952 (1992).
14. HEK293 cells (American Type Culture Collection) were grown in Dulbecco’s modified Eagle’s medium (DMEM) supplemented with 10% fetal bovine serum. Cells were transfected using calcium phosphate coprecipitation. Stably transfected cells were isolated following selection on 0.5% geneticin or 0.2% Zeocin (Invitrogen, Carlsbad, CA).

15. D. L. Kaufman et al., *J. Biol. Chem.* **270**, 15877 (1995).
16. Radioligand binding assays were carried out using  $^3$ H-diprenorphine as previously described (6, 12).
17. Intact cells were reacted with disulfide-linked biotin to label receptors in the plasma membrane. After the indicated period of agonist exposure, surface biotin was cleaved by exposure of cells to glutathione and the internalized (glutathione-resistant) pool of receptors was detected in immunoprecipitates. “100%” refers to the biotinylated receptor signal present in cells after initial labeling and without further manipulation. “strip” refers to biotinylated cells that were reacted with glutathione without other manipulations, demonstrating the efficiency with which biotin can be cleaved from surface receptors. Detailed methods are available as supporting materials on Science Online.
18. J. L. Whistler, P. Tsao, M. von Zastrow, *J. Biol. Chem.* **276**, 34331 (2001).
19. Receptors present in the plasma membrane of living cells were labeled with M1 mouse anti-FLAG IgG2b (Sigma) and then surface-labeled cells were incubated at 37°C as described in the materials and methods (17) and were fixed using paraformaldehyde. Labeled receptors were localized relative to LAMP1 and LAMP2 or HA-GASP using appropriate mouse IgG1 antibodies and dual-color fluorescence microscopy.
20. The R DOR was constructed by replacing the 30 COOH-terminal residues of the DOR with the 38 corresponding residues of the MOR.
21. Membrane adenylyl cyclase assays were performed as previously described (9) to measure the ability of opioid receptors to inhibit adenylyl cyclase activity upon agonist rechallenge of a membrane fraction prepared from receptor-expressing cells after the ligand incubations.
22. The COOH-terminal tail of murine DOR-1 (residues 337 to 391) was used to identify interacting clones, and the interacting clones were isolated from a 293 cell-derived cDNA library (Clontech, Palo Alto, CA) using the Gal4-based MATCHMAKER system (Clontech). A total of  $2.5 \times 10^6$  recombinants were screened.
23. M. Suyama, T. Nagase, O. Ohara, *Nucleic Acids Res.* **27**, 338 (1999).
24. U. Klein, M. T. Ramirez, B. K. Kobilka, M. von Zastrow, *J. Biol. Chem.* **272**, 19099 (1997).
25. In vitro translated cGASP bound to GST-tail constructs in the following order: DOR = D MOR  $\gg$  R DOR > MOR > GST. The same order of binding strength was obtained using binding of in vitro-translated full-length GASP.
26. S. F. Altschul et al., *Nucl. Acids Res.* **25**, 3389 (1997).
27. The GASP antibody was prepared commercially by Zymed (South San Francisco, CA) to the 15 COOH-terminal residues of GASP using standard methods.
28. The GASP sequence encodes an acidic protein with a predicted mass of 156.8 kD. In vitro transcription and translation of this clone yielded a protein with an apparent mass of  $\sim$ 190 kD when resolved by SDS-polyacrylamide gel electrophoresis (SDS-PAGE) in tris-glycine buffer and  $\sim$ 170 kD in Mops buffer. We have not investigated this observation in detail. However, differences between actual and apparent molecular weights estimated by SDS-PAGE are not uncommon. TATA-binding protein, for example, has a predicted molecular weight of 30 kD but electrophoreses with an apparent molecular weight of 45 kD (29).
29. M. G. Peterson, N. Tanese, B. F. Pugh, R. Tjian, *Science* **248**, 1625 (1990).
30. cGASP was tagged at the NH<sub>2</sub>-terminus using pEGFP-C1 (Clontech). Coimmunoprecipitations were performed without crosslinking from lysates prepared using 0.1% Triton X-100; 150 mM NaCl; 25 mM KCl; and 10 mM tris-HCl (pH 7.4) containing 1  $\mu$ M leupeptin, 1  $\mu$ M pepstatin A, 1  $\mu$ M aprotinin, and 2.5  $\mu$ M Pefabloc SC.
31. Myelin basic protein (MBP)-DOR cytoplasmic tail and MBP-lacZ fusion proteins were expressed and purified on amylose resin. Full-length GASP probe was generated by in vitro transcription and translation as previously described (25) and incubated with 15  $\mu$ g MBP-fusion protein. For competition, GST-cGASP

- was bacterially expressed and purified on glutathione agarose, and the purified protein was eluted with glutathione and quantified. Eluted GST-cGASP was added to the MBP-DOR slurry just before addition of in vitro-translated full-length GASP probe.
32. Cells expressing only endogenous GASP and cells overexpressing GFP-cGASP (~40 times the level of endogenous GASP as estimated by immunoblotting) were grown to 80% confluency and treated with 5  $\mu$ M EGF in DMEM for the indicated times or left untreated. Cells were washed with phosphate-buffered saline (PBS), and the EGF receptor was immunoprecipitated with rabbit anti-EGFR-affinity resin (Santa Cruz Biotechnology, Santa Cruz, CA), separated by SDS-PAGE, and immunoblotted with goat anti-EGFR antibodies to EGFR (Santa Cruz Biotechnology), followed by horseradish peroxidase (HRP)-conjugated secondary antibody to goat (Jackson ImmunoResearch, Malvern, PA) and development with ECL reagents (Amersham, Piscataway, NJ).
  33. D. A. Heck, D. B. Bylund, *J. Pharmacol. Exp. Ther.* **282**, 1219 (1997).
  34. G. Innamorati, H. M. Sadeghi, N. T. Tran, M. Birnbaumer, *Proc. Natl. Acad. Sci. U.S.A.* **95**, 2222 (1998).
  35. M. von Zastrow, B. K. Kobilka, *J. Biol. Chem.* **267**, 3530 (1992).
  36. M. Cong *et al.*, *J. Biol. Chem.* **276**, 45145 (2001).
  37. R. M. Gage, K. A. Kim, T. T. Cao, M. von Zastrow, *J. Biol. Chem.* **276**, 44712 (2001).
  38. L. Hicke, *Trends Cell Biol.* **9**, 107 (1999).
  39. A. Marchese, J.L. Benovic, *J. Biol. Chem.* **276**, 45509 (2001).
  40. S. K. Shenoy, P. H. McDonald, T. A. Kohout, R. J. Lefkowitz, *Science* **294**, 1307 (2001).
  41. U. E. Petaja-Repo *et al.*, *J. Biol. Chem.* **276**, 4416 (2001).
  42. K. Chaturvedi, P. Bandari, N. Chinen, R. D. Howells, *J. Biol. Chem.* **276**, 12345 (2001).
  43. We thank P. Chu for expert assistance in carrying out

the yeast two-hybrid screen; U. Klein for valuable advice on the interaction cloning strategy and for performing initial GST binding assays; P. Tsao for insightful discussion and assistance in early studies of the GASP interaction; G. Vargas for providing the GST-D4 tail construct; and H. Bourne, H. Deacon, R. Edwards, A. Finn, R. Kelly, D. Ron, and M. Waldhoer for helpful discussion and critical reading of the manuscript. Supported by research grants from NIH (M.v.Z.) and funds provided by the state of California for medical research on alcohol and substance abuse (J.L.W.). J.L.W. is supported by a NARSAD young investigator award from the Staglin family and received an individual NRSA from NIH.

**Supporting Online Material**

[www.sciencemag.org/cgi/content/full/297/5581/615/DC1](http://www.sciencemag.org/cgi/content/full/297/5581/615/DC1)

Materials and Methods

26 April 2002; accepted 13 June 2002

## Identification of *Bphs*, an Autoimmune Disease Locus, as Histamine Receptor H<sub>1</sub>

Runlin Z. Ma,<sup>1,2</sup> Jianfeng Gao,<sup>3</sup> Nathan D. Meeker,<sup>2</sup> Parley D. Fillmore,<sup>2</sup> Kenneth S. K. Tung,<sup>4</sup> Takeshi Watanabe,<sup>5</sup> James F. Zachary,<sup>2</sup> Halina Offner,<sup>6</sup> Elizabeth P. Blankenhorn,<sup>7</sup> Cory Teuscher<sup>3\*</sup>

*Bphs* controls *Bordetella pertussis* toxin (PTX)-induced vasoactive amine sensitization elicited by histamine (VAASH) and has an established role in autoimmunity. We report that congenic mapping links *Bphs* to the histamine H<sub>1</sub> receptor gene (*Hrh1/H1R*) and that H1R differs at three amino acid residues in VAASH-susceptible and -resistant mice. *Hrh1*<sup>-/-</sup> mice are protected from VAASH, which can be restored by genetic complementation with a susceptible *Bphs/Hrh1* allele, and experimental allergic encephalomyelitis and autoimmune orchitis due to immune deviation. Thus, natural alleles of *Hrh1* control both the autoimmune T cell and vascular responses regulated by histamine after PTX sensitization.

autosomal dominant locus known as *Bphs* (10). *Bphs* was one of the first nonmajor histocompatibility complex-linked genes shown to be involved in susceptibility to multiple autoimmune diseases (10). Previously, we mapped *Bphs* on mouse chromosome 6 using backcross populations generated with susceptible SJL/J and resistant C3H/HeJ and CBA/J mice (10). As the first step in positionally cloning *Bphs*, we generated a panel of recombinant, interval-specific congenic lines using marker-assisted selection to introgress the SJL/J *Bphs* allele (*Bphs*<sup>s</sup>) onto the C3H/HeJ background (11). These lines were tested for susceptibility to VAASH (Table 1). The results establish that *Bphs* resides within an interval  $\leq 1$  cM between *D6Mit107* and *D6Mit41*, encompassing *Hrh1*. Additionally, homozygous and heterozygous C3H.SJL-*Bphs* line D mice are as sensitive to VAASH as SJL/J, over a dose range of 6.25 to 100 mg/kg (table S1). This is consistent with dominance and a lack of gene dosage effect at this locus (10).

It is known that the histamine H<sub>1</sub> receptor antagonist mepyramine can block VAASH in rats (12), and, because *Hrh1* resides within the interval encoding *Bphs*, *Hrh1* was a candidate gene for *Bphs*. Therefore, we cloned and sequenced the *Hrh1* alleles from cDNA samples of 14 inbred strains of mice (table S2). With the exception of C3H/HeJ and CBA/J, all mouse strains are susceptible to VAASH. *Hrh1* sequences from susceptible and resistant mouse strains exhibited multiple, single nucleotide polymorphisms. However, among these polymorphisms, only three led to distinct and concordant amino acid changes in the predicted sequence (L263P, M313V, and S331P), all of which distinguish C3H/HeJ and CBA/J from all other strains of mice (fig. S1).

The identity of *Hrh1* as *Bphs* was further verified using C57BL/6-*Hrh1*<sup>-/-</sup> (13) and C57BL/6-*Hrh2*<sup>-/-</sup> (14) mice. *Hrh1*<sup>-/-</sup> mice were completely resistant to VAASH, whereas *Hrh2*<sup>-/-</sup> mice were fully susceptible (Table

PTX is a major virulence factor of *B. pertussis*, the causative agent of Whooping Cough (1). The holotoxin is a hexameric protein that conforms to the  $\alpha\beta$  model of bacterial exotoxins (2). The  $\alpha$  subunit is an adenosine diphosphate (ADP)-ribosyl transferase, which affects signal transduction by ribosy-

lation of the  $\alpha$  subunit of trimeric G<sub>i</sub> proteins, whereas the  $\beta$  oligomer binds cell surface receptors on a variety of mammalian cells (2, 3). PTX, when administered in vivo, elicits a range of responses including disruption of glucose regulation, leukocytosis, adjuvant activity, increased vascular permeability associated with alteration of blood-tissue barrier functions, and sensitization to vasoactive amines (VAAS) (4, 5). The latter two phenotypes are the result of PTX-induced changes in vascular endothelial cells. Inbred strains of mice differ in susceptibility to vasoactive amine challenge after PTX sensitization in that genetically susceptible strains die from hypotensive and hypovolemic shock, whereas resistant strains do not (4). Additionally, the genetic control of susceptibility to lethal shock is vasoactive amine specific (4) and is mediated through a variety of mechanisms (6–9).

Hypersensitivity to histamine after PTX sensitization (VAASH) is controlled by an

<sup>1</sup>Laboratory Animal Center, Institute of Genetics, Chinese Academy of Sciences, Beijing, China 100101.

<sup>2</sup>Department of Veterinary Pathobiology, University of Illinois at Urbana-Champaign, Urbana, IL 61802-6178, USA.

<sup>3</sup>Department of Medicine, University of Vermont, Burlington, VT 05405-0068, USA.

<sup>4</sup>Department of Pathology, University of Virginia, Charlottesville, VA 22908-0001, USA.

<sup>5</sup>Medical Institute of Bioregulation, Kyushu University, Fukuoka, Japan.

<sup>6</sup>Department of Neurology, Oregon Health and Science University and Neuroimmunology Research, Veterans Affairs Medical Center, Portland, OR 97201-3098, USA.

<sup>7</sup>Department of Microbiology and Immunology, MCP Hahnemann University, Philadelphia, PA 19129-1129, USA.

\*To whom correspondence should be addressed. E-mail: cteusche@zoo.uvm.edu